

Article

Microstructure and Magnetic Properties of Ce₁₄Fe₇₈Co₂B₆ Nanopowders Prepared by Ball Milling at Low Temperature

Marian Grigoras , Mihaela Lostun , Firuta Borza, Marieta Porcescu, George Stoian  and Nicoleta Lupu 

National Institute of Research & Development for Technical Physics, 700050 Iasi, Romania; fborza@phys-iasi.ro (F.B.); porcescu@phys-iasi.ro (M.P.); gstoian@phys-iasi.ro (G.S.); nicole@phys-iasi.ro (N.L.)
* Correspondence: mgrigoras@phys-iasi.ro (M.G.); mlostun@phys-iasi.ro (M.L.)

Abstract: Ce₁₄Fe₇₈Co₂B₆ nanopowders with hard-magnetic properties have been successfully prepared by ball milling at low temperatures in liquid nitrogen. The morphology, structure, and magnetic properties of Ce₁₄Fe₇₈Co₂B₆ powders have been investigated using scanning electron microscopy, X-ray diffraction, and vibrating sample magnetometry, respectively. It was found that powder ball milling at low temperature in liquid nitrogen, has the advantage that the oxidation of powders is inhibited and the particles rapidly reach nanometric dimensions. In comparison to the Ce₁₄Fe₇₈Co₂B₆ powders prepared by ball milling at room temperature, the powders milled at low temperature present a more uniform particle size and no rare-earth oxides, which leads thus to remarkable magnetic properties. The nanocrystalline Ce₁₄Fe₇₈Co₂B₆ powders with optimum characteristics, prepared at low temperature, have the size of 153 nm or less, present a coercivity of 5.1 kOe, and a saturation magnetization of 113 emu/g after milling for 6 h at low temperature. Low temperature milling may become a promising technique for the fabrication of high performance powders used for permanent magnets preparation.



Citation: Grigoras, M.; Lostun, M.; Borza, F.; Porcescu, M.; Stoian, G.; Lupu, N. Microstructure and Magnetic Properties of Ce₁₄Fe₇₈Co₂B₆ Nanopowders Prepared by Ball Milling at Low Temperature. *Magnetochemistry* **2021**, *7*, 160. <https://doi.org/10.3390/magnetochemistry7120160>

Academic Editor: Jean Ebothe

Received: 17 November 2021
Accepted: 8 December 2021
Published: 10 December 2021

Publisher's Note: MDPI stays neutral with regard to jurisdictional claims in published maps and institutional affiliations.



Copyright: © 2021 by the authors. Licensee MDPI, Basel, Switzerland. This article is an open access article distributed under the terms and conditions of the Creative Commons Attribution (CC BY) license (<https://creativecommons.org/licenses/by/4.0/>).

Keywords: Ce-FeCo-B nanopowders; low-temperature milling; magnetic properties; microstructure

1. Introduction

Due to their excellent magnetic properties, Nd-Fe-B magnets, have been widely applied in numerous modern devices including traction motors for hybrid vehicles, wind turbines, magnetic resonance imaging machines, consumer electronics, and so on [1–3]. The Nd-Fe-B magnets seriously rely on the addition of rare earth elements (RE) such as dysprosium (Dy), praseodymium (Pr), and terbium (Tb) in order to improve the magnetic properties at temperatures above 200 °C [4]. However, Dy, Pr, Tb, and Nd are considered critical elements and while the consumption of RE-based magnets is increasing dramatically, this results in the depletion of the critical RE elements. Furthermore, mining and extraction of RE elements causes various environmental problems [5–7]. Hence, there is a rising demand for alternative magnets that do not rely on critical RE elements [8]. Ce-based rare-earth alloys have attracted considerable attention recently as good candidates for the preparation of permanent magnets without critical rare earths, mainly owing to the abundance and low cost of Ce element in rare-earth resources [9–12]. However, the Curie temperature of Ce-Fe-B alloy ($T_c \sim 152$ °C) is lower than that of Nd-Fe-B alloy so that T_c enhancement solutions should be considered. Substitution of Fe by Co was found to enhance the T_c in Ce-Fe-B alloys [13]. There are several methods used for the preparation of permanent magnets such as sintering, spark plasma sintering, and hot pressing, which involve powder compaction. All these methods have in common the use of raw material in the form of powders. It is well established that the particle size of the powders is an extremely important parameter that influences the magnetic performance of magnets. For this reason, the choice of the processing route and its optimization being necessary. The coercivity of magnetic powders depends very much on the grain size and morphology. High-performance magnets with high coercivity are obtained when the grains of hard

magnetic phase are at nanometer scale [14,15]. Therefore, a smaller powder size is required in order to obtain permanent magnets with good magnetic properties. High-energy ball milling, jet milling, Hydrogenation-Disproportionation-Desorption-Recombination (HDDR) methods as well as combinations of these methods have been used to prepare powders with dimensions down to approximately 0.33 μm [16,17]. In order to further refine the powders down to nanoscale, surfactant-assisted ball milling (SABM) was employed [18,19]. For example, Chakka et al. [20] prepared SmCo, and NdFeB powders with a size smaller than 30 nm by using the SABM technique in the presence of oleic acid, oleylamine, and heptanes as surfactants. However, due to their nanometric size, magnetic powders can oxidize easily during washing-removal of the surfactant. In addition, the milling temperature has been proven to be one of the key experimental parameters that has remarkable influence on the magnetic properties of powders. For example, Liu et al. [21] have shown that SmCo₅ nanoflakes with improved magnetic properties such as increased remanence ratio and higher coercivity can be achieved by lowering milling temperature. Fang et al. [22] fabricated Sm-Fe-N powders with enhanced magnetic performance at low temperatures by using ball milling without using solvents or surfactants. Nanocrystalline Nd-Fe-B particles with the size of 40 nm or less have been obtained by combining the HDDR with cryo-milling technique [23].

The aim of our work is to propose a new route for the preparation of magnetic nanopowders with good magnetic characteristics from Ce₁₄Fe₇₈Co₂B₆ ribbon precursors, by using the ball milling technique at low temperatures, and to study their magnetic properties for the fabrication of high performance permanent magnets.

2. Materials and Methods Experimental

Ce₁₄Fe₇₈Co₂B₆ melt-spun ribbons were prepared (National Institute of Research and Development for Technical Physics, Iasi, Romania) by melt-spinning technique and subsequently annealed in vacuum at 680 °C for 20 min to obtain crystalline ribbons as raw material. The ribbons were then crushed and grounded in an agate jar down to less than 400 μm , in an argon glove box. Five grams of coarse powders were placed in each of the two stainless steel vials of a RETSCH PM 200 planetary ball mill (Retsch GmbH, Haan, Germany). The powder from one vial was used for ball milling at low temperature, while the powder from the second vial was used for ball milling at room temperature. Both sets of samples were milled for up to 6 h, the ball-to-powder weight ratio being 10:1. The low temperature milling process was carried out in the following steps: cooling the milling vial in a liquid nitrogen bath for 3 min, introducing then a certain quantity of liquid nitrogen into the vial until the balls are completely covered, followed by milling for 10 min. The vial cooling, the introduction of liquid nitrogen, and the milling processes are repeated alternatively for a total milling time of 6 h. The temperature of the vial was kept below 0 °C during the entire ball milling process. For the room temperature milling process, nitrogen gas was used as protective gas in the vial. Both sets of powders, low temperature or room temperature milled, were collected in the glove box under argon protection. The phase evolution following these processes was examined by X-ray diffraction (XRD) using a Bruker AXS D8-Advance diffractometer (Bruker AXS GmbH, Karlsruhe, Germany) with Cu Ka radiation. To observe the morphology of the powders, scanning electron microscopy (FIB/FE-SEM Cross-Beam Carl Zeiss NEON 40 EsB) (Carl Zeiss AG, Oberkochen, Germany) was employed. Particle size was determined using the ImageJ software. Magnetic measurements were performed using a vibrating sample magnetometer (LakeShore 7410) (Lake Shore Cryotronics, Inc., Westerville, OH, USA).

3. Results and Discussions

Figure 1 shows the X-ray diffraction patterns of the Ce₁₄Fe₇₈Co₂B₆ powders milled for different periods of time at room temperature and low temperature, respectively. The pattern of the starting powders is also presented for comparison. For the case of powders milled at room temperature (Figure 1a), it can be observed that they present nanocrystalline

structure, with a mixture of $\text{Ce}_2(\text{FeCo})_{14}\text{B}$, CeFe_2 , and Ce_2O_3 phases. When the ball-milling time increases from 1 to 6 h, the $\text{Ce}_2(\text{FeCo})_{14}\text{B}$ peaks of the main phase become broader while the intensity decreases monotonically. This indicates that some amorphous phases may arise due to disorder and dislocations caused by the milling process. At the same time, the Ce_2O_3 peaks become more pronounced indicating that slight oxidation may occur during the prolongation of the preparation process. The gradual milling down to smaller particle size leads to a high surface to volume ratio, which allows them to be easily oxidized. The rare earth oxides are also easy to be formed even at room temperature [24] and extremely easy to be formed at elevated temperatures [25,26] in an air environment. The presence of a small content of oxygen is almost inevitable in the milling medium. The presence of oxygen connected with the increase in the system temperature due to collision and friction during the milling process speeds up the oxidation process.

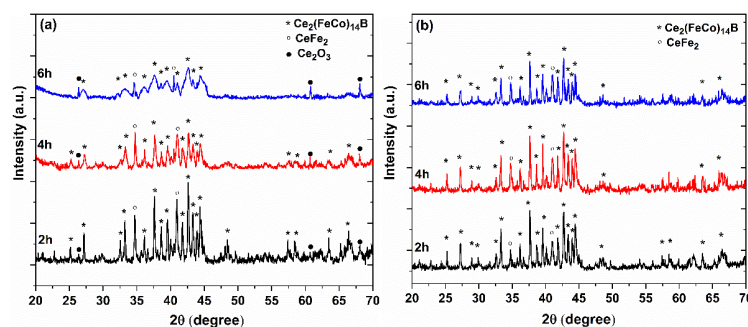


Figure 1. XRD patterns of $\text{Ce}_{14}\text{Fe}_{78}\text{Co}_2\text{B}_6$ powders milled at room (a) and at low (b) temperatures.

The powders milled at low temperature reveal a nanocrystalline structure consisting of a mixture of $\text{Ce}_2(\text{FeCo})_{14}\text{B}$ and CeFe_2 phases (Figure 1b). The low temperature milling present the advantage that it can delay the increase of the system temperature that will, effectively, inhibit the oxidation of powders. Indeed, no obvious diffraction peaks of rare earth oxides have been detected in the XRD patterns, indicating that the as-prepared low temperature powders have been more efficiently protected from oxidation during the fabrication and examination processes. Moreover, it can be observed that the low temperature milled powders appear to preserve the aspect of the XRD patterns. The reason for such good stability of the hard phase and the prevention against oxidation can be related to the presence of liquid nitrogen, as shown by other authors [27,28].

Evolution of size and morphology of milled powders was investigated as a function of the milling time by scanning electron microscopy (SEM). Figure 2 presents the SEM images of $\text{Ce}_{14}\text{Fe}_{78}\text{Co}_2\text{B}_6$ powders after milling at room temperature (a, b) and low temperature (c, d) for 2 and 6 h, respectively. During the milling process, the powder is subjected to repeated plastic deformations due to the collision of the milling balls. The minimum particle size that can be reached during mechanical milling is decided by the balance between particle breaking and cold welding. It is well known that, at low temperatures, the breaking process dominates due to the fragility of the material, while at high temperatures, the predilection for cold welding increases. For a milling time of 2 h there is a certain similarity in the morphology of both room-temperature milled and low-temperature milled powders (Figure 2a,c), the difference appearing only in the size of powders. Thus, the particle milled at room temperature has a size of 2.3 μm or less, while the particles milled at low temperature have a size of 530 nm or less. At the beginning of the milling process, at the defects and the displacements sites, the internal tension due to the collisions leads to a rapid breakdown of the powders giving an irregular aspect of the milled powders. For a milling time of 6 h (Figure 2b,d), an obvious difference between the morphology of the two powders can be observed.

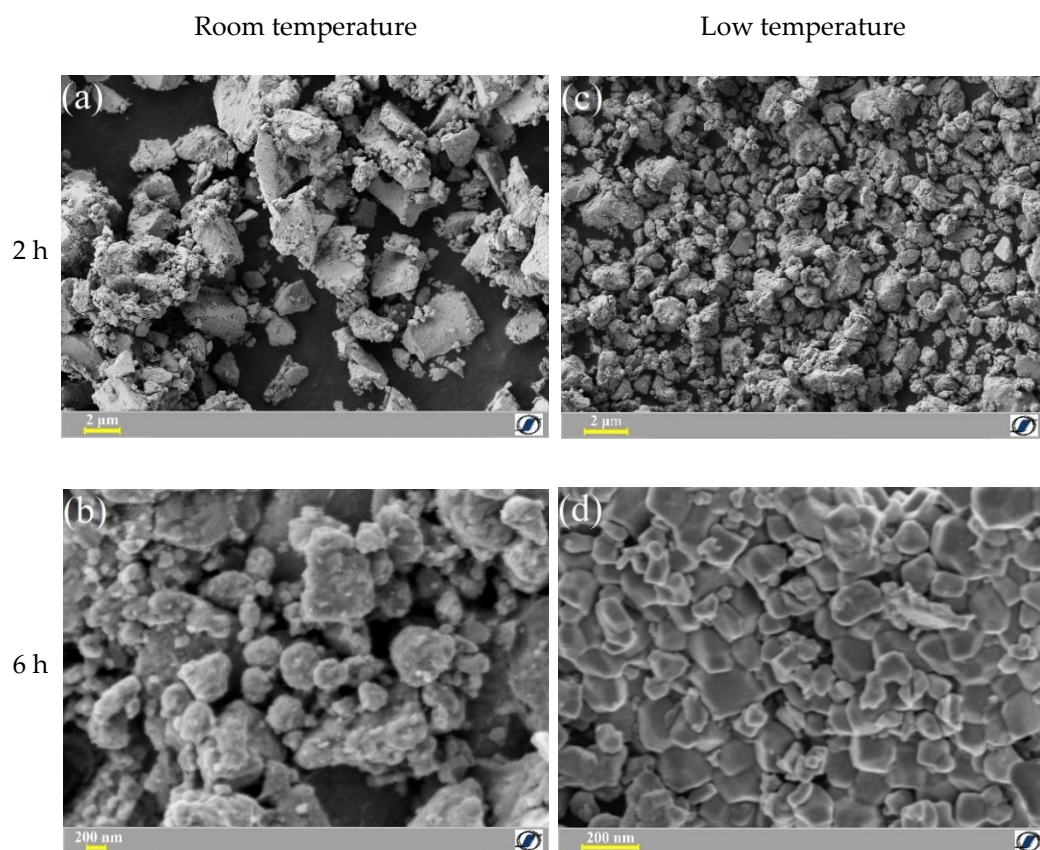


Figure 2. SEM images of $Ce_{14}Fe_{78}Co_2B_6$ powders prepared by ball-milling for 2 and 6 h at room temperature (a,b) and at low temperature (c,d).

As compared to the powders milled at room temperature, the powders milled at low temperature presents a smoother aspect due to the fact that, in the second phase of milling, the micro-cracks start from the grains boundary, as a result of crystal mismatch between grains, propagating along the grain boundaries. These powders have a much smaller particle size (153 nm for the low temperature vs. 460 nm for the room temperature milled powders) and a more homogeneous distribution of particle size. In contrast, the powders milled at room temperature have an irregular shape and an inhomogeneous size distribution, which indicate that cold-welding and particles agglomeration occur during the milling process.

Figure 3 shows the mean particle size of $Ce_{14}Fe_{78}Co_2B_6$ powders versus milling time.

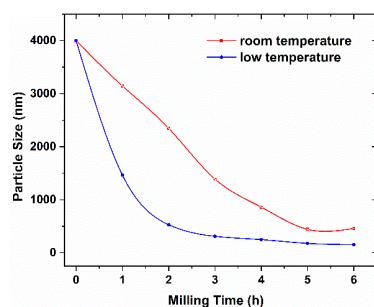


Figure 3. The mean particle sizes of $Ce_{14}Fe_{78}Co_2B_6$ powders milled at room and low temperature for different milling times.

The general trend is that as the milling time increases, the particle size decreases, as determined using the Image J software. However, the powders milled at room temperature

show a decrease in particle size with increasing the milling time up to 5 h, after which their size increases with milling time due to rewelding of crushed particles so that the size of the particles increases. For the powders milled at low temperature, the particle size first drops rapidly and then, after up to 2 h, slowly decreases. For the same milling time, the average size of the powders milled at low temperature is always smaller than the size of those milled at room temperature, which is consistent with the results presented in Figure 2. This behavior is expected due to the fact that at low temperatures the alloy becomes brittle and easier to be broken into fine particles.

Figure 4 shows the hysteresis loops of the powders prepared at both low and room temperatures for different milling times.

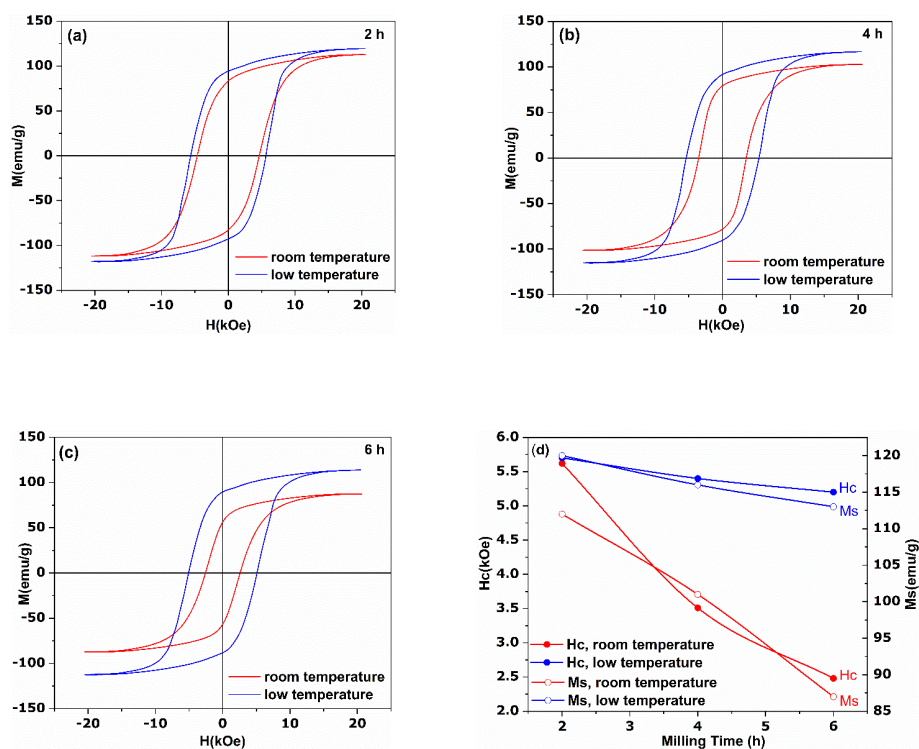


Figure 4. Hysteresis loops of the $\text{Ce}_{14}\text{Fe}_{78}\text{Co}_2\text{B}_6$ powder milled at low and room temperatures for 2 h (a), 4 h (b), 6 h (c), and evolution of their H_c and M_s vs. milling time (d).

All loops present a single-phase like magnetization behavior, indicating no second magnetic phases in the particles. This is in agreement with the XRD patterns (Figure 1), which show that besides the $\text{Ce}_2(\text{FeCo})_{14}\text{B}$ main phase, a secondary CeFe_2 phase (which is paramagnetic over 230 K [29]) is formed. Additionally, an oxide phase (Ce_2O_3) appears in the powders milled at room temperature. With the increase in milling time, both saturation magnetization and coercivity of sample prepared at room temperature decrease. For example, the powders having under 2.3 μm particles, the 850 nm particles and the 460 nm particles have the saturation magnetization of 112, 101, and 87 emu/g, and coercivities of 5.62, 3.51, and 2.48 kOe, respectively. The decrease in coercivity as the particle size decreases was also observed by other authors [30,31]. Lower coercivity can be attributed to the cumulative effect of (i) increased number of defects in particles that can cause low-energy nucleation sites [32], (ii) micro-strains induced by milling [23], as well as (iii) partial amorphization during milling [20]. The degradation of saturation magnetization may be related to the occurrence of both amorphous and Ce_2O_3 phases, as indicated by XRD investigations (Figure 1). The powders prepared at low temperature present a much slighter decrease in coercivity, remanence and in saturation magnetization, as compared to the samples prepared at room temperature (Figure 4d), maintaining the hard-magnetic character of the raw material. Thus, the powders milled 2 h at low temperature have

$H_c = 5.7$ kOe, $M_s = 120$ emu/g and $M_r = 95$ emu/g, while the powders milled for 6 h present $H_c = 5.2$ kOe, $M_s = 113$ emu/g, and $M_r = 89$ emu/g. The reasons for the slighter decrease in coercivity can be attributed to a lesser extent to the first two reasons mentioned above for powders milled at room temperature, i.e., increased number of defects and microstrains. Partial amorphization during low temperature milling cannot be considered as a reason for the decrease in coercivity, as no widening of the diffraction peaks is observed in any of the XRD patterns, as in the case of powders milled at room temperature. Therefore, we can conclude that low temperature milling is beneficial to achieve better magnetic performance for powders with nanometer dimensions.

4. Conclusions

In summary, $Ce_{14}Fe_{78}Co_2B_6$ nanopowders have been successfully prepared using ball milling at room temperature and low temperatures in liquid nitrogen. It is found that the milling temperature has a great influence on the crystal structure, morphology, and magnetic properties of the $Ce_{14}Fe_{78}Co_2B_6$ powders. Low temperature milling has the following advantages (i) accelerates the decrease in particle size due to increased brittleness, (ii) inhibits the cold welding during the ball milling process, and (iii) protects particle from oxidation. As a result, the $Ce_{14}Fe_{78}Co_2B_6$ powders milled at low temperature exhibit better magnetic properties compared to those prepared at room temperature. The best magnetic properties, coercivity of 5.1 kOe and saturation magnetization of 113 emu/g, were obtained in $Ce_{14}Fe_{78}Co_2B_6$ nanopowders having the size of about 153 nm, obtained after 6 h of milling at low temperatures. Our results indicate that the low temperature milling may serve as a promising technique for the fabrication of high performance powders used for permanent magnets preparation.

Author Contributions: Conceptualization, funding acquisition, resources, investigation, result discussion, writing—original draft, M.G.; Sample preparation, experimental design, data analysis, writing—original draft, M.L.; Data curation, formal analysis, investigation, equipment assistance, G.S.; investigation, data analysis, result discussion, M.P.; Writing—original draft and editing, language proofreading, F.B.; Supervision, methodology, result discussion N.L. All authors have read and agreed to the published version of the manuscript.

Funding: This work was supported by a grant of the Romanian Ministry of Research, Innovation and Digitization, CNCS/CCCDI-UEFISCDI, project number PN-III-P2-2.1-PED-2019-2054, within PNCDI III.

Institutional Review Board Statement: Not applicable.

Informed Consent Statement: Not applicable.

Data Availability Statement: Data supporting the reported results are available at the request of the appropriate author.

Conflicts of Interest: The authors declare no conflict of interest. The funders had no role in the design of the study; in the collection, analyses, or interpretation of data; in the writing of the manuscript, or in the decision to publish the results.

References

1. Gutfleisch, O.; Willard, M.A.; Brück, E.; Chen, C.H.; Sankar, S.G.; Liu, J.P. Magnetic Materials and Devices for the 21st Century: Stronger, Lighter, and More Energy Efficient. *Adv. Mater.* **2011**, *23*, 821–842. [[CrossRef](#)] [[PubMed](#)]
2. Matsuura, Y. Recent development of Nd–Fe–B sintered magnets and their applications. *J. Magn. Magn. Mater.* **2006**, *303*, 344–347. [[CrossRef](#)]
3. Coey, J.M.D. Permanent magnets: Plugging the gap. *Scr. Mater.* **2012**, *67*, 524–529. [[CrossRef](#)]
4. Marinescu, M.; Chiriac, H.; Grigoras, M. Magnetic properties of bulk nanocomposite permanent magnets based on NdDyFeB alloys with additions. *J. Magn. Magn. Mater.* **2005**, *290–291*, 1267–1269. [[CrossRef](#)]
5. Schreiber, A.; Marx, J.; Zapp, P.; Hake, J.F.; Voßenkaul, D.; Friedrich, B. Environmental Impacts of Rare Earth Mining and Separation Based on Eudialyte: A New European Way. *Resources* **2016**, *5*, 32. [[CrossRef](#)]
6. Rare Earth Elements-Purification, Separation and Recycling. Available online: <https://www.ivl.se/download/18.76c6e08e1573302315f3b85/1480415049402/C211.pdf> (accessed on 9 December 2021).

7. How Rare-Earth Mining Has Devastated China's Environment. Available online: <https://earth.org/rare-earth-mining-has-devastated-chinas-environment/> (accessed on 9 December 2021).
8. Pathak, A.K.; Gschneidner, K.A., Jr.; Khan, M.; McCallum, R.W.; Pecharsky, V.K. High performance Nd-Fe-B permanent magnets without critical elements. *J. Alloy. Compd.* **2016**, *668*, 80–86. [[CrossRef](#)]
9. Zhu, M.G.; Li, W.; Wang, J.D.; Zheng, L.Y.; Li, Y.F.; Zhang, K.; Feng, H.B.; Liu, T. Influence of Ce Content on the Rectangularity of Demagnetization Curves and Magnetic Properties of Re-Fe-B Magnets Sintered by Double Main Phase Alloy Method. *IEEE Trans. Magn.* **2014**, *50*, 1000104. [[CrossRef](#)]
10. Grigoras, M.; Lostun, M.; Stoian, G.; Herea, D.D.; Chiriac, H.; Lupu, N. Microstructure and magnetic properties of $Ce_{10+x}Fe_{84-x}B_6$ nanocrystalline ribbons versus preparation conditions. *J. Magn. Magn. Mater.* **2017**, *432*, 119–123. [[CrossRef](#)]
11. Gabay, A.M.; Martín-Cid, A.; Barandiaran, J.M.; Salazar, D.; Hadjipanayis, G.C. Low-cost $Ce_{1-x}Sm_x(Fe, Co, Ti)_{12}$ alloys for permanent magnets. *AIP Adv.* **2016**, *6*, 056015. [[CrossRef](#)]
12. Zhao, W.; Liu, Y.; Li, J.; Shi, Q. Phase and microstructure formation of strip-cast Ce-Fe-B alloys for multi-phases RE-Fe-B magnets. *Intermetallics* **2019**, *114*, 106606. [[CrossRef](#)]
13. Skoug, E.J.; Meyer, M.S.; Pinkerton, F.E.; Tessema, M.M.; Haddad, D.; Herbst, J.F. Crystal structure and magnetic properties of $Ce_2Fe_{14-x}Co_xB$ alloys. *J. Alloy. Compd.* **2013**, *574*, 552–555. [[CrossRef](#)]
14. Skomski, R.; Coey, J.M.D. Giant energy product in nanostructured two-phase magnets. *Phys. Rev. B* **1993**, *48*, 15812–15816. [[CrossRef](#)]
15. Fukada, T.; Matsuura, M.; Goto, R.; Tezuka, N.; Sugimoto, S.; Une, Y.; Sagawa, M. Evaluation of the Microstructural Contribution to the Coercivity of Fine-Grained Nd-Fe-B Sintered Magnets. *Mater. Trans.* **2012**, *53*, 1967–1971. [[CrossRef](#)]
16. Nakamura, M.; Matsuura, M.; Tezuka, N.; Sugimoto, S.; Une, Y.; Kubo, H.; Sagawa, M. Preparation of ultrafine jet-milled powders for Nd-Fe-B sintered magnets using hydrogenation–disproportionation–desorption–recombination and hydrogen decrepitation processes. *Appl. Phys. Lett.* **2013**, *103*, 022404. [[CrossRef](#)]
17. McGuinness, P.J.; Zhang, X.J.; Yin, X.J.; Harris, I.R. Hydrogenation, disproportionation and desorption (HDD): An effective processing route for Nd₂Fe₁₄B-type magnets. *J. Less. Common. Met.* **1990**, *158*, 359–365. [[CrossRef](#)]
18. Akdogan, N.G.; George, C.H.; David, J.S. Novel Nd₂Fe₁₄B nanoflakes and nanoparticles for the development of high energy nanocomposite magnets. *Nanotechnology* **2010**, *21*, 295705. [[CrossRef](#)] [[PubMed](#)]
19. Cui, B.; Zheng, L.; Li, W.; Liu, J.; Hadjipanayis, G. Single-crystal and textured polycrystalline Nd₂Fe₁₄B flakes with a submicron or nanosize thickness. *Acta Mater.* **2012**, *60*, 1721–1730. [[CrossRef](#)]
20. Chakka, V.M.; Altuncevhahir, B.; Jin, Z.Q.; Li, Y.; Liua, J.P. Magnetic nanoparticles produced by surfactant-assisted ball milling. *J. Appl. Phys.* **2006**, *99*, 08E912. [[CrossRef](#)]
21. Liu, L.; Zhang, S.; Zhang, J.; Liu, J.P.; Xia, W.; Du, J.; Yan, A.; Yi, J.; Li, W.; Guo, Z. Highly anisotropic SmCo₅ nanoflakes by surfactant-assisted ball milling at low temperature. *J. Magn. Magn. Mater.* **2015**, *374*, 108–115. [[CrossRef](#)]
22. Fang, Q.; An, X.; Wang, F.; Li, Y.; Du, J.; Xia, W.; Yan, A.; Liu, J.P.; Zhang, J. The structure and magnetic properties of Sm-Fe-N powders prepared by ball milling at low temperature. *J. Magn. Magn. Mater.* **2016**, *410*, 116–122. [[CrossRef](#)]
23. Zhang, F.; Liu, Y.; Li, J.; Wang, R. Ultrafine nanocrystalline NdFeB prepared by cryomilling with HDDR process. *J. Alloy. Compd.* **2018**, *750*, 401–408. [[CrossRef](#)]
24. Kùlah, E.; Marot, L.; Steiner, R.; Romanyuk, A.; Jung, T.A.; Wàckerlin, A.; Meyer, E. Surface chemistry of rare-earth oxide surfaces at ambient conditions: Reactions with water and hydrocarbons. *Sci. Rep.* **2017**, *7*, 43369. [[CrossRef](#)] [[PubMed](#)]
25. Li, Y.; Evans, H.; Harris, I.; Jones, I. The Oxidation of NdFeB Magnets. *Oxid. Met.* **2003**, *59*, 167–182. [[CrossRef](#)]
26. Pragnell, W.M.; Williams, A.J.; Evans, H.E. The oxidation of SmCo magnets. *J. Appl. Phys.* **2008**, *103*, 07E127. [[CrossRef](#)]
27. Tiwary, C.S.; Kashyap, S.; Biswas, K.; Chattopadhyay, K. Synthesis of pure iron magnetic nanoparticles in large quantity. *J. Phys. D Appl. Phys.* **2013**, *46*, 385001. [[CrossRef](#)]
28. Katiyar, N.K.; Biswas, K.; Tiwary, C.S. Cryomilling as environmentally friendly synthesis route to prepare nanomaterials. *Int. Mater. Rev.* **2021**, *66*, 493–532. [[CrossRef](#)]
29. Zhang, M.; Liu, Y.; Li, Z.; Peng, L.; Shen, B.; Hu, F.; Sun, J. Magnetization process of nanocrystalline mischmetal-Fe-B ribbons. *J. Alloy. Compd.* **2016**, *688*, 1053–1057. [[CrossRef](#)]
30. Poudyal, N.; Rong, C.-B.; Liu, J.P. Effects of particle size and composition on coercivity of Sm-Co nanoparticles prepared by surfactant-assisted ball milling. *J. Appl. Phys.* **2010**, *107*, 09A703. [[CrossRef](#)]
31. Li, W.; Hu, X.; Cui, B.; Yang, J.; Han, J.; Hadjipanayis, G. Magnetic property and microstructure of single crystalline Nd₂Fe₁₄B ultrafine particles ball milled from HDDR powders. *J. Magn. Magn. Mater.* **2013**, *339*, 71–74. [[CrossRef](#)]
32. Yi, M.; Zhang, H.; Gutfleisch, O.; Xu, B.-X. Multiscale Examination of Strain Effects in Nd-Fe-B Permanent Magnets. *Phys. Rev. Appl.* **2017**, *8*, 014011. [[CrossRef](#)]